coatings

MDPI

Article

Research on Drag Reduction by Coating the Inner Wall of Hydraulic Pipeline

Xue Wang [1], Junjie Zhou [1,2,*], Wenbo Liao [1] and Shihua Yuan [1]

[1] School of Mechanics and Vehicles, Beijing Institute of Technology, Beijing 100081, China; 3120185221@bit.edu.cn (X.W.); bit10007liao@163.com (W.L.); bit10007zhou@163.com (S.Y.)
[2] Institute of Frontier Technology, Beijing Institute of Technology, Beijing 250101, China
* Correspondence: bit_zhou50082@163.com

Abstract: This study employs computational fluid dynamics (CFD) simulations to investigate the effect of wall roughness on linear loss in circular pipelines. It specifically addresses hemispherical roughness, focusing on how changes in spacing influence linear loss, a critical determinant of fluid motion within pipelines. The simulations further assess the impact of these variables on flow characteristics, laying a theoretical groundwork for drag reduction and pipeline design improvement. Results indicate that increased spacing between roughness elements reduces the differential pressure at both pipeline ends. The dimensionless spacing value of 30 stabilizes this pressure, suggesting a limit to further changes. Additionally, a rise in roughness height at this spacing exacerbates differential pressure, highlighting a proportional relationship between roughness dimensions and linear loss—greater roughness leads to higher linear loss. Applying a nickel-plated coating on the inner wall significantly lowers roughness, thereby reducing linear loss.

Keywords: roughness; CFD numerical simulation; linear loss; drag reduction

Citation: Wang, X.; Zhou, J.; Liao, W.; Yuan, S. Research on Drag Reduction by Coating the Inner Wall of Hydraulic Pipeline. *Coatings* **2024**, *14*, 802. https://doi.org/10.3390/coatings14070802

Academic Editors: Matic Jovičević-Klug, Patricia Jovičević-Klug, László Tóth and Georgios Skordaris

Received: 30 April 2024
Revised: 21 June 2024
Accepted: 24 June 2024
Published: 27 June 2024

1. Introduction

The influence of wall roughness on boundary layer flow within pipelines has garnered significant academic interest, contributing extensively to the body of research on single-phase turbulent flow through channels with various roughness geometries [1–3]. Research has extensively explored how different roughness shapes affect fluid flow in pipelines [4]. Oktarina et al. [5] investigated the impact of cylindrical surface roughness on fluid flow characteristics, finding that increased roughness disrupts flow and enhances vortex formation at greater distances. Similarly, Ashmawy [6] studied the effects of surface roughness on stress in fluid flows, demonstrating a marked decrease in flow velocity as longitudinal corrugation roughness increases. Yu et al. [7] analyzed flow resistance in pipelines, highlighting vortices induced by surface roughness and introduced a new method for calculating the friction coefficient. Memento et al. [8] performed experiments to determine how pipeline diameter and surface roughness influence the friction coefficient in fluid flows, noting that both inlet conditions and surface roughness impact the friction coefficient across different pipeline diameters. They also observed a significant increase in pressure drop magnitude with decreasing pipeline size. Further, Oktarina et al. [9] examined the effects of wall roughness on resistance to fluid transport in nanopores, revealing a more pronounced impact in smaller nanotubes. Du et al. [10] used scanning electron microscopy (SEM) to create a three-dimensional model of surface roughness and explored its effect on flow resistance in microtubes, finding that increased roughness significantly raises flow resistance, especially when relative roughness exceeds 3%. Yang et al. [11] investigated flow resistance along rough boundaries in open channels and pipelines, affirming the boundary shear stress summation principle's applicability, which consistently aligns with experimental data in depicting the friction coefficient in pipelines. Lastly, Song et al. [12] studied

the impact of surface roughness on flow fields and pressure drops in circular pipelines, developing a theoretical model to quantify roughness effects on fluid dynamics.

Research on the impact of small hemispherical roughness, whether regularly or randomly distributed, on channel walls remains sparse. Wu et al. [13] performed direct numerical simulations (DNS) of turbulent flows over hexagonally packed hemispheres, establishing a scaling relationship between universal wall shear stress variance and average size, which supports the development of wall models for large eddy simulations (LES). Iyer et al. [14] investigated the effects of discrete and distributed roughness through DNS, finding that roughness can induce coherent streamwise vortices and enhance fluid transition. Philip [15] conducted experimental studies on single hemispherical roughness on a flat plate within a zero-pressure gradient laminar boundary layer, focusing on the Strouhal number-related behavior of "hairpin" vortices induced by roughness, their role in the development of a turbulent boundary layer, and their dependency on inflection point instability. Zhou et al. [16] combined DNS with the immersed boundary method to explore boundary layer flow transition induced by three-dimensional roughness, revealing the evolution of hairpin vortices and secondary vortex structures. A subsequent simulation demonstrated quantitative consistency with experimental data using two-component Particle Image Velocimetry (PIV). Michele et al. [17] examined vortex structure in turbulent boundary layers over sparse hemispherical roughness, confirming the presence of vortex packets in the outer flow layer. Prahladh [18] utilized DNS to study the transition from laminar to turbulent flow in high-speed laminar boundary layers caused by discrete hemispherical roughness. Observations indicated that flow with a Mach number of 8.23 remained laminar downstream of the roughness, while transitions occurred at lower Mach numbers. Caviezel et al. [19] conducted DNS and LES of fully developed turbulent flow in channels with smooth-walled and hemispherical roughness at shear Reynolds numbers (Re) of 180 and 400, finding that the friction factor decreases with increasing Reynolds number and roughness spacing but increases significantly with roughness height. Interestingly, the random distribution of these cells had a relatively minor effect on both the friction factor and average velocity. Additionally, strategic placement of roughness facilitated immediate lateral movement of flow within the wall layer, effectively enhancing fluid transport. Qin et al. [20] performed molecular dynamics simulations to assess the effects of various roughness shapes, including hemispherical, on nanofluid flow in nanochannels. Results indicated that surface roughness reduces the range of density fluctuation near nanochannel walls, with triangular roughness having the most significant impact on nanofluid flow characteristics.

Regarding fluid transport in pipelines, linear loss is a critical factor that cannot be overlooked, primarily stemming from the interaction between the fluid and the pipeline wall [21]. This interaction significantly impacts the efficiency and performance of the fluid conveyance system. Recognizing the importance of minimizing linear losses is essential for the design and operation of fluid transport systems [22]. Optimization of pipeline design, including adjustments to pipeline diameter and surface roughness, along with the implementation of drag reduction devices [23], can facilitate this. Such measures not only enhance system energy efficiency and reduce operational costs but also extend the lifespan of pipelines and decrease maintenance requirements [24]. Consequently, this study employs numerical simulation to examine the effects of the height and spacing of hemispherical roughness, regularly distributed along channel walls, on linear loss. The objective is to diminish drag by reducing wall roughness [25].

This paper investigates the impact of inner wall roughness on the drag reduction performance of turbulent hydraulic oil flow (Re > 5000) in hydraulic steel pipelines using computational fluid dynamics (CFD) for numerical simulation. The study focuses on the enhancement of drag reduction by applying an inner wall surface coating, thereby reducing roughness. Initially, hemispherical roughness units are modeled on the inner surface of the circular pipe using a 1/4 circular pipeline model to decrease computational demands. The study also explores how variations in roughness spacing influence drag

reduction, thereby advancing our understanding of roughness in pipeline hydrodynamics. Furthermore, a nickel-plated coating is applied to the inner wall to reduce roughness and minimize linear losses, providing insights for optimizing pipeline design and reducing fluid resistance. This investigation builds on findings from Reference [26], which demonstrated that a nickel-plated metal coating on the inner walls of hydraulic steel pipelines effectively reduces linear loss in laminar flow. Extending these findings, this study explores turbulence reduction by applying a similar nickel-plated coating, aiming to decrease wall roughness in hydraulic steel pipelines. The numerical simulations assess the influence of coating thickness variations on roughness modification and the consequent drag reduction, explaining these effects through changes in the height and morphology of the roughness.

2. Numerical Simulation of Pipeline Drag Reduction

This study employs three-dimensional numerical simulations to explore turbulent fluid flow through horizontally oriented, straight circular pipelines using Ansys Fluent software. The Re is calculated based on the inlet flow rate, provided that the piping parameters are established. Simulations are performed at various wall roughness levels to measure the pressure differential across the pipeline. The objective of this research is to enhance understanding of the characteristics of turbulent oil flow within straight pipelines. To this end, the simulations focus on the effect of varying wall roughness on the pressure differential at both ends of the pipeline, thereby gathering relevant data to assess pipeline linear loss and optimize pipeline design.

2.1. Physical Model

The length of the inlet section required to achieve fully developed flow is critical as it signifies the distance necessary to initiate turbulence within the conduit. In the context of a horizontal circular pipeline, this distance is represented by the length over which the fluid transitions from laminar to turbulent flow due to friction and other influencing factors. This length typically spans several times the diameter of the pipeline. The determination of this length takes into account factors such as pipeline geometry, fluid characteristics, and the Re. An accurate evaluation of the length of the inlet section in fully developed flow is essential for effective fluid system design, analysis, and a comprehensive understanding of fluid dynamics. The length of the inlet section, which marks the commencement of fully developed flow in a pipeline, correlates with the Re, as described by Equations (1) and (2) [27], which characterize turbulent states.

$$E_l = 4.4 \cdot \mathrm{Re}^{1/6} (\mathrm{Re} > 4000) \tag{1}$$

$$L = E_l \cdot d \tag{2}$$

In Equation (1), E_l represents the inlet section length factor, and L denotes the length of the inlet turbulence, while d indicates the pipeline diameter. Accompanying this description is a reference chart that illustrates the necessary inlet section length to achieve a fully developed flow. Figure 1 depicts a schematic of a fluid dynamics simulation for a horizontal circular pipeline, illustrating the concept of a fully developed flow and the turbulent inlet section. This schematic helps determine the minimum distance fluid must travel through the pipeline to reach the state referred to as "fully developed". In such a flow, the velocity profile remains constant along the pipeline axis, indicating no further changes in the flow dynamics.

The length of the inlet segment prior to the computational domain is crucial for the accuracy of the computations. An insufficient length in the entrance section leads to inadequate development of turbulence within the pipeline. In this study, the inlet section was measured to be approximately 0.7 m.

This study utilizes a quarter-circle pipeline model with uniformly distributed roughness to define the computational domain. Subsequently, the pressure differential between the two ends of the horizontally oriented pipeline is calculated. Comparative analyses

between the complete circular pipeline model and the quarter-circle pipeline model consistently yield congruent results, indicating that the quarter-circle model effectively reduces the computational workload without compromising accuracy. This model is illustrated in Figure 2, where the pipeline is 1.2 m in length and has a radius of 20 mm. The model's length was chosen based on the 0.7 m length of the inlet section. In this study, a 0.5 m segment following the inlet section is selected as the subject of analysis to calculate the pressure difference across this portion of the pipeline. The spacing in the flow direction, denoted as *sf*, and the circumferential spacing, indicated as *sc*, are established. Furthermore, the height of the hemispherical roughness is represented as *h*. The fluid within the tube is specified as hydraulic oil with a density of 870 kg/m^3 and a dynamic viscosity of 0.04 kg/(m·s) at a temperature of 40 °C, as detailed in Table 1.

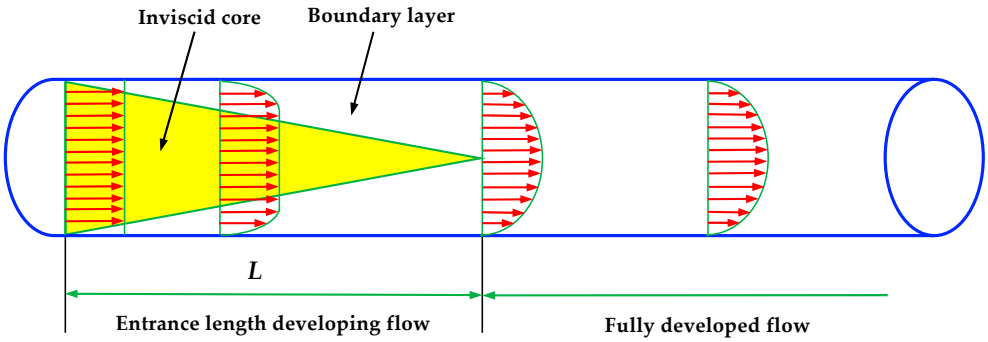

Figure 1. Attainment of full development of the inlet section length.

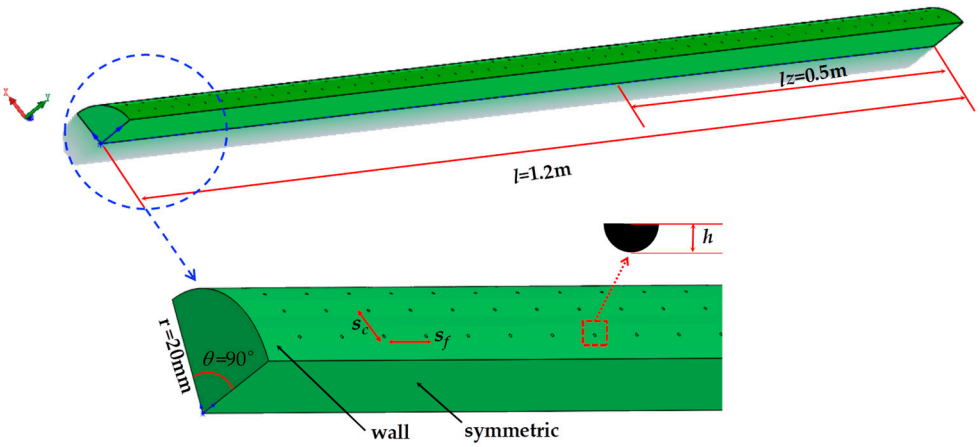

Figure 2. Quarter-circle pipeline calculation model with hemispherical roughness.

Table 1. Parameters of numerical simulation.

ρ (kg/m^3)	T (°C)	μ (kg/m·s)	v (m/s)	Re
870	40	0.04	6	5220

2.2. Mesh Generation

The resistance to fluid flow in a pipeline is predominantly caused by the interaction between the fluid and the pipeline wall, which generates a significant velocity gradient near the wall. To address this, the mesh near the wall, particularly around rough areas and along the wall-normal at their ends, is refined to ensure adequate resolution of these rough features. In this study, the flow regime, characterized by a low Re, requires a y+ value of approximately 1 to effectively resolve the boundary layer. The y+ is a dimensionless number that quantifies the distance from the wall where the fluid's viscous effects become

significant. This method allows for a more precise capture of the near-wall flow dynamics. The near-wall boundary layer is modeled with at least eight mesh layers, employing a mesh growth rate of 1.2. The mesh growth rate describes the degree to which the sizes of adjacent meshes vary. This study rigorously validated grid convergence through detailed pressure and velocity analyses across various piping systems with grid densities ranging from 2 to 12 million cells. It utilized Richardson extrapolation in conjunction with Computational Geometric Information (CGI) techniques. The findings indicate a crucial observation: the discrepancy between predicted and actual pressure and velocity readings narrows to less than 1% at a grid size of 10 million cells. This suggests that enhancements in simulation accuracy become incremental beyond this grid density, confirming that a configuration of 10 million cells is sufficient for stable and accurate simulations of piping systems. Furthermore, CGI calculation outcomes support this conclusion, showing consistent pressure and velocity distributions across different grid densities, particularly at higher densities where variations stabilize. This underscores the effectiveness of using an 11 million grid size for precise hydrodynamic simulations of piping systems, optimizing computational resources. The mesh is divided as in Figure 3 and the hemispherical roughness elements are encrypted.

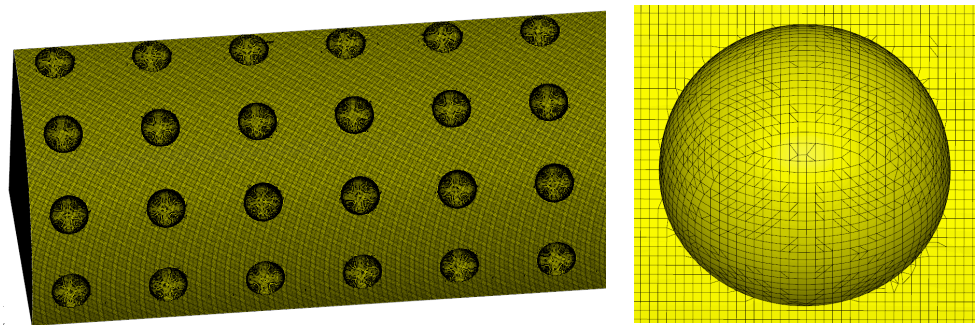

Figure 3. Rough cell meshing.

2.3. Boundary Conditions

The boundary conditions for the flow field simulation are meticulously defined to accurately reflect the state of the fluid at the beginning of the simulation. The inlet boundary condition specifies an inlet velocity of 6 m/s to precisely characterize the initial fluid dynamics. Conversely, the outlet boundary is established as a pressure boundary to effectively model the evolution of fluid pressure throughout the channel. The inner wall roughness of the pipeline is represented as a wall surface to faithfully simulate the interaction between the fluid and the rough surface. For turbulent flows, it is essential to allow turbulence to fully develop, ensuring uniformity in flow field characteristics both longitudinally and spanwise. This uniformity is critical for determining the accuracy of the simulation results, particularly in capturing the subtleties of flow in various directions. To minimize the effect of sidewalls on the flow field, the side boundaries are configured as symmetric. This setup prevents sidewall interference and facilitates a more realistic simulation of pipeline turbulence.

2.4. Turbulence Numerical Simulation

Investigating the flow fields over rough surfaces requires a detailed examination of the structure of the turbulent boundary layer. For this purpose, Reynolds-Averaged Navier-Stokes (RANS) simulations, which balance computational efficiency with the capability to capture micro flow field details, are particularly suitable. Therefore, RANS simulations are conducted in this study to analyze the flow field. Efficient computation is achieved by time-averaging the transient Navier-Stokes equations and utilizing the classical RNG turbulence model. The RNG k-ε model refines the computation of the turbulence length scale, which enhances the precision of turbulent viscosity estimations compared to the traditional k-ε

model. This refinement is particularly effective in simulations of near-wall flows, where it accurately predicts complex turbulence phenomena adjacent to walls. Furthermore, the RNG k-ε model excels at forecasting flow separation phenomena, such as protrusions, by incorporating the impact of localized turbulence intensity variations on the flow. This aspect is crucial for examining wall-related studies and understanding the influence of geometric features on flow dynamics. Additionally, the augmented numerical stability and reliability of the RNG k-ε model ensure dependable outcomes in simulations involving complex boundary conditions and variable flow scenarios. Precise meshing is required to accurately delineate flow within the boundary layer; insufficient mesh refinement can lead to inaccuracies in predicting the flow field, especially near walls.

The Reynolds-averaged numerical simulation is performed for this calculation, with the governing equation detailed in Reference [28] expressed as follows:

Continuity Equation:

$$\frac{\partial \rho}{\partial t} + \frac{\partial}{\partial x_i}(\rho u_i) = 0 \tag{3}$$

Ds-averaged Navier-Stokes Equation:

$$\frac{\partial \overline{U}_i}{\partial t} + \overline{U}_j \frac{\partial \overline{U}_i}{\partial x_j} = -\frac{1}{\rho}\frac{\partial \overline{P}}{\partial x_i} + \frac{1}{\rho}\frac{\partial}{\partial x_j}\left(\mu \frac{\partial \overline{U}_i}{\partial x_j} - \rho \overline{u}_i \overline{u}_j\right) \tag{4}$$

The initial conditions are defined as [28]: The initial turbulence intensity is defined as:

$$I \approx 0.16 \mathrm{Re}^{-\frac{1}{8}} \tag{5}$$

The initial turbulent kinetic energy is defined as:

$$k = \frac{3}{2}(\overline{U}I)^2 \tag{6}$$

The initial turbulence dissipation rate is defined as:

$$\varepsilon = C_\mu{}^{\frac{3}{4}} \frac{k^{\frac{3}{2}}}{l} \tag{7}$$

The $\bar{U}$ is mean velocity, C_μ = 0.09 is an empirical constant, l = 0.07L, and L is the characteristic length.

The discretization method employs a pressure-based SIMPLEC algorithm to enhance numerical stability by refining the pressure term in the discretized equations, thus mitigating the risk of numerical instability associated with the SIMPLE algorithm. Furthermore, a second-order upwind discretization scheme is utilized to improve accuracy and stability, offering significant advantages over the first-order scheme. Setting the convergence criterion at 10^{-5} ensures that the numerical simulation incrementally approaches the correct solution through iterative refinement, thereby avoiding excessive computation while meeting practical requirements [29].

3. Calculation of Different Roughness Parameters

The model incorporates hemispherical roughness arranged in a regular pattern on the wall. The selection of hemispherical roughness is informed by the findings from extensive domestic and international research cited in the introduction. This research indicates that hemispherical roughness is suitable for modeling the roughness of the inner walls of circular tubes, hence the adoption of this shape in the model. Key factors influencing fluid loss along the pipeline include the spacing and height of the roughness elements. By varying the spacing of these roughness elements, their impact on fluid flow within the pipeline can be quantified. We conducted separate analyses of the spacing and height of these roughness elements to clarify their effects on the inner wall surface and linear fluid

loss. Consequently, the hemispherical roughness model addresses the localized effects of wall roughness on fluid dynamics, and adjusting these roughness characteristics enables the simulation of fluid loss along the pipeline.

3.1. Equal Spacing Goughness Calculation

In the near-wall region, wall conditions significantly influence flow velocity and distribution, highlighting the need for a detailed model to accurately represent fluid behavior due to pronounced interactions with roughness. Conversely, in the outer-wall region, the impact of roughness on flow is minimal, permitting the use of a simplified model to estimate fluid behavior further from the wall. Consequently, the model incorporating hemispherical roughness effectively accounts for the localized effects of wall roughness on fluid flow, facilitating the simulation of fluid loss along the pipeline by adjusting roughness characteristics.

The spacing of the roughness results in a slightly higher pressure differential at the pipeline end under irregular conditions compared to regular distribution conditions. This study contrasts irregular roughness distributions along the circumferential and flow directions, revealing that a regular distribution condition is more advantageous for minimizing losses along the pipeline. To further the research on the effects of a rough inner wall on fluid flow, we propose the introduction of another parameter: the spacing between roughness units in both the flow direction and the circumferential direction, denoted as *sf* and *sc* respectively. When *sf* equals *sc*, it indicates that the spacing of roughness units is uniform in both the longitudinal and circumferential directions. With the roughness height set to 0.03 mm and relative roughness at 0.00075, the flow in the pipeline is calculated for the dimensionless roughness spacings of $sf/\varepsilon = sc/\varepsilon$. Figure 4 illustrates the dimensionless roughness, and the corresponding values of differential pressure for equally spaced roughness.

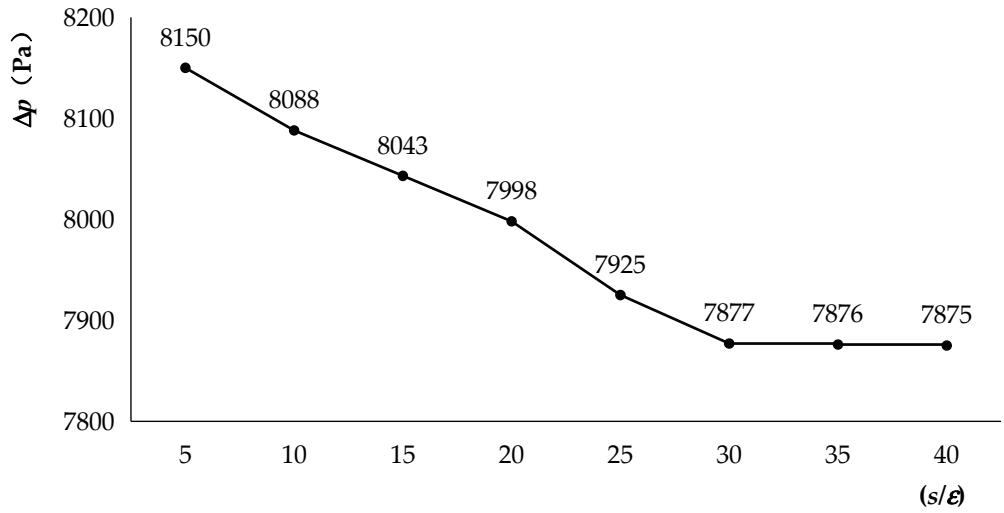

Figure 4. Differential pressure values for equidistant roughness.

The analysis of the calculation results depicted in Figure 4 demonstrates a nuanced relationship between surface roughness spacing and differential pressure. Specifically, an inverse relationship is observed for the dimensionless spacings less than 30: as the roughness spacing increases, the differential pressure decreases. Beyond this point, the rate of decrease in differential pressure slows, followed by a stabilization where the rate of pressure drop becomes very gradual and approaches a horizontal level. According to the Darcy-Weisbach equation (Equation (8)), the friction resistance coefficient is calculated as illustrated in Figure 5. As shown in Figure 5, the coefficient of frictional resistance along the pipeline begins to decrease gradually as roughness spacing increases. After the

the dimensionless spacing reaches 30, there are no further changes, indicating that the maximum value of the frictional resistance coefficient has been reached.

$$h_f = \lambda \frac{l}{d} \frac{v^2}{2g} \tag{8}$$

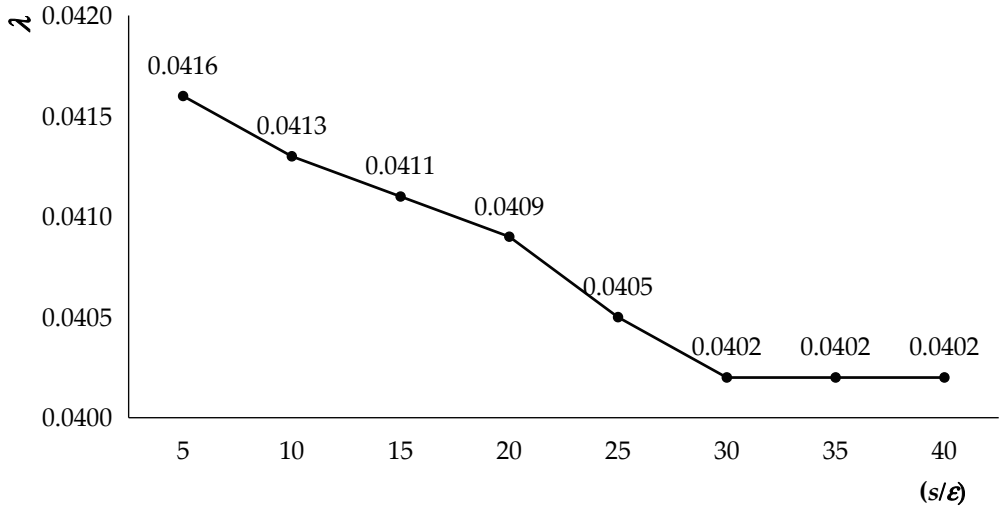

Figure 5. Friction resistance coefficient of different spacing.

Based on the roughness spacing determined in Figure 4, a consistent spacing of 30 was established. Differential pressure values between the two ends of the pipeline were calculated for varying roughness heights, with the results displayed in Figure 6. These roughness heights are based on the actual measurements taken from the hydraulic pipeline, hence the defined roughness heights. Observations from Figure 6 reveal that pressure loss in rough pipelines significantly exceeds that in smooth pipelines. Transitioning from the smooth to the rough tube, the rate of differential pressure increase significantly escalates. As roughness varies from 0.00025 to 0.00075, the rate of increase slows; however, further increasing the roughness causes the pressure growth rate to accelerate. As roughness increases from 0.00025 to 0.000125, there is a corresponding rise in differential pressure, consistent with the relationship described by the Darcy-Weisbach equation. The resistance coefficients for different roughness levels are shown in Table 2, illustrating that resistance coefficients increase with roughness.

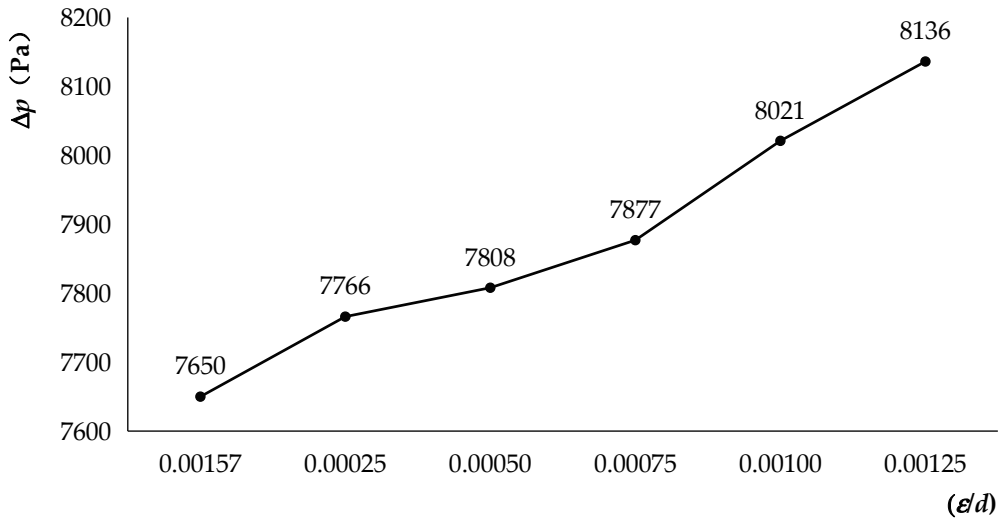

Figure 6. Differential pressure values for varied roughness height.

Table 2. Friction resistance coefficient of different roughness.

Frictional (λ)	Absolute Roughness (ε)	Relative Roughness (ε/d)
0.0391	smooth	-
0.0397	10 μm	0.00025
0.0399	20 μm	0.00050
0.0402	30 μm	0.00075
0.0401	40 μm	0.00100
0.0416	50 μm	0.00125

Figure 6 demonstrates that differential pressure in pipelines escalates with increased wall roughness, especially under turbulent flow conditions characterized by low Re. From a surface engineering perspective, applying nickel-metal coatings provides a solution by creating a smoother inner pipeline surface, thus diminishing the friction between the fluid and the wall. This smoothing effect is achieved by leveling out surface irregularities. The thickness of the coating plays a crucial role in reducing frictional losses; however, an excessively thick coating may restrict the pipeline's internal diameter, subsequently elevating flow resistance. Conversely, an overly thin coating may not sufficiently smooth out the rough patches on the inner wall. Therefore, identifying the optimal coating thickness is essential for ensuring sufficient smoothness without significantly reducing the pipeline's effective diameter. This investigation into drag reduction involved examining the effects of various coating thicknesses on longitudinal losses, with evaluations based on differential pressure variations at both pipeline ends. The findings from these numerical analyses are presented in Figure 6, with a baseline roughness of 0.00075.

Figure 7 illustrates the differential pressure values at both ends of a pipeline under various coating thicknesses. The data show that uncoated pipelines exhibit higher differential pressures, highlighting the efficacy of coatings in reducing these pressures. A marked decline in differential pressure is observed as coating thickness increases from 10 μm to 30 μm, indicating that thicker coatings improve the smoothness of the pipeline's internal surface, thereby reducing turbulence and associated pressure losses. The differential pressure value for pipelines with coatings is lower than that of uncoated pipelines under equivalent conditions of roughness height. However, at a coating thickness of 30 μm, the differential pressure in the pipeline exceeds that of a pipeline with a smooth inner surface. These findings emphasize the value of coatings as a strategic measure to enhance hydraulic efficiency and reduce operational costs in pipeline systems.

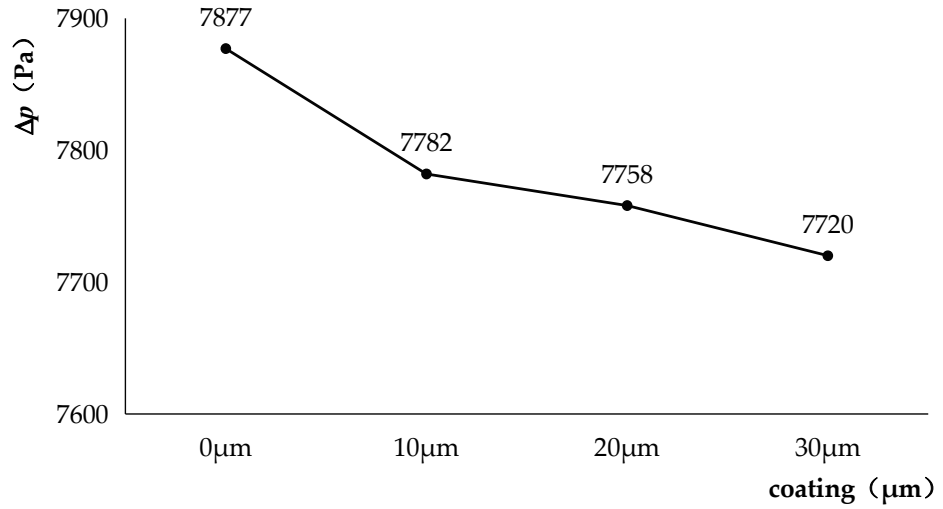

Figure 7. Pressure differential under different coating thickness.

3.2. Analysis of Drag Reduction Rate

The formula for calculating the drag reduction rate is detailed in Equation (9) [26]. According to this formula, there is a defined relationship between the loss incurred along the pipeline and the pressure difference. Consequently, this study employs the pressure difference to evaluate the drag reduction rate. Thus, the formula for the drag reduction rate can be equated to Equation (9):

$$\eta = \frac{\Delta h - \Delta h_{\text{coating}}}{\Delta h} \tag{9}$$

The evaluation of drag reduction facilitated by the coating involved analyzing changes in the pressure differential as defined in Equation (8). The drag reduction rate, indicative of the coating's effectiveness, was subsequently calculated. These results were compiled and illustrated in Figure 8, providing a clear reference for assessing and analyzing the drag reduction data in the context of this study.

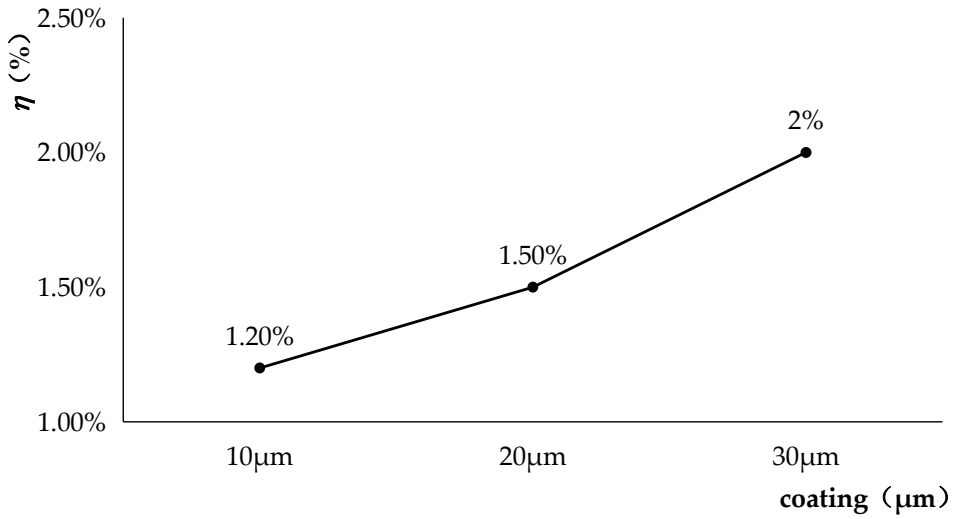

Figure 8. Drag reduction rate for different thicknesses of coatings.

Data analysis indicates that drag reduction decreases as coating thickness increases. A significant reduction of 2% was observed in samples with a 30 μm coating thickness. In contrast, samples with a 10 μm coating thickness exhibited the least reduction. Therefore, for practical applications where drag minimization is critical, maintaining a coating thickness of 30 μm is advisable.

4. Analysis of the Coating's Drag Reduction Mechanism

This study introduces a numerical simulation method which demonstrates that a coating thickness of 30 μm yields a notably smoother surface, significantly reducing frictional resistance within pipelines. The coating's effectiveness stems from its dual functionality: masking surface roughness and regulating the thickness of the viscous sublayer. The former directly reduces surface roughness, while the latter substantially affects the fluid's frictional resistance against the pipe wall. Thus, the coating not only diminishes roughness and modulates the viscous sublayer thickness but also enhances flow gradients and markedly decreases frictional resistance, reducing overall energy consumption.

The study explores the impact of coating thickness on the hydraulic performance of pipelines by evaluating various thicknesses. Specifically, coatings of 10 μm and 20 μm proved insufficient to conceal the 30 μm surface roughness of the pipeline wall. This inadequate coverage adversely affected the viscous sublayer, diminishing local flow velocity and increasing fluid friction. Conversely, a 30 μm coating effectively smoothes the rough surface of the pipeline and optimizes the flow path, thereby significantly reducing flow

instability and turbulence and enhancing drag reduction. Nonetheless, the implications of utilizing excessively thick coatings were also considered. While a 30 μm coating adequately covers underlying roughness and improves overall smoothness, the material's intrinsic roughness may generate higher differential pressure than that observed in a completely smooth-lined pipe. This observation highlights the necessity to balance the coating's thickness and material properties to optimize pipeline performance while minimizing adverse hydraulic effects.

Velocity vector charts for both smooth and rough pipeline walls are presented in Figures 9 and 10. The disparity in fluid flow velocity gradients between soft and rough wall surfaces significantly influences hydraulic dynamics. Smooth wall surfaces exhibit a slight velocity gradient, indicating a gradual transition in velocity among fluid molecules, which enhances the stability of fluid flow. In contrast, rough wall surfaces display a more pronounced velocity gradient, suggesting abrupt changes in velocity among fluid molecules, thereby increasing susceptibility to turbulence and eddies, which contribute to unstable flow. Friction on smooth pipeline walls is minimal, leading to relatively low energy losses, whereas friction on rough walls is heightened, resulting in increased energy losses. A coating thickness of 30 μm effectively transforms rough wall surfaces into smoother ones.

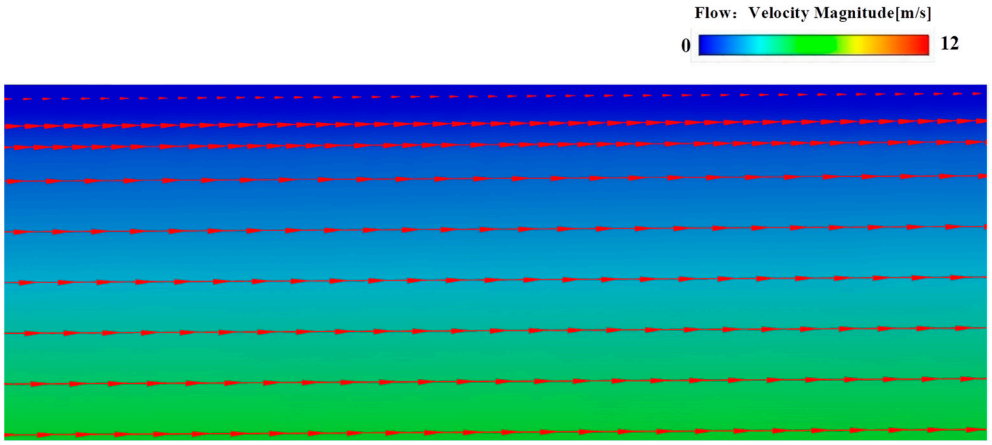

Figure 9. Smooth wall surface velocity.

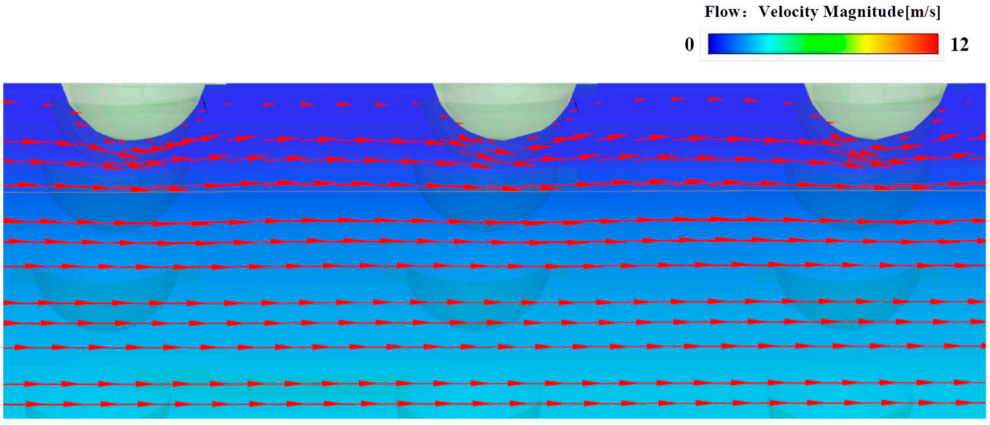

Figure 10. Rough wall surface velocity.

Figures 11 and 12 illustrate the surface roughness of velocity clouds before and after the application of a coating, respectively. The analysis reveals that the height of roughness decreases following the application of the coating to the rough wall surface, with the shape no longer retaining its initial hemispherical form. This modification lowers the fluid velocity gradient across the roughness surface, leading to smoother fluid flow within the pipeline. The reduced gradient facilitates a more uniform interaction among fluid molecules, thereby

diminishing fluid fluctuations and eddies. Consequently, this smoother flow significantly lowers the differential pressure within the pipeline, enabling a more efficient passage of fluid. Thus, pipelines with coatings exhibit lower linear losses and reduced differential pressure values compared to their uncoated counterparts, given the same roughness height.

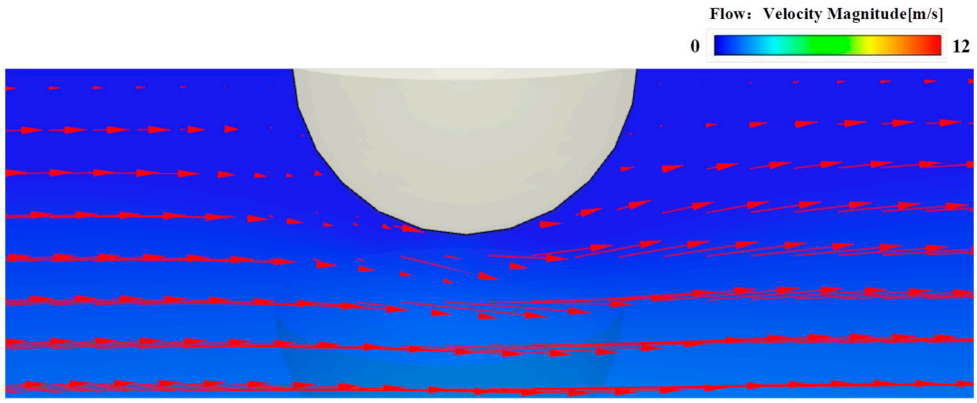

Figure 11. Uncoated rough surface velocity.

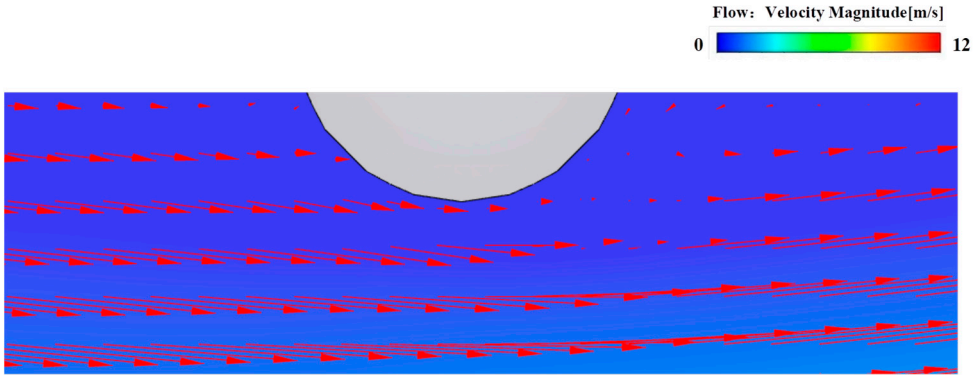

Figure 12. Rough surface velocity with coating.

5. Conclusions

This article examines the critical parameters influencing losses along turbulent circular pipelines, focusing on roughness spacing and coating thickness. It analyzes the effects of these parameters on turbulence and friction losses. The main findings include: Numerical simulations indicate that the characteristics of roughness, specifically the spacing, significantly impact fluid flow losses. By appropriately adjusting the roughness spacing, friction and turbulence losses can be substantially reduced. Stability in differential pressure values is achieved when roughness spacing is increased to 30. The study also investigates the effect of coating thickness on drag reduction. Results confirm that a 30 μm coating thickness optimizes drag reduction, achieving up to a 2% decrease. This thickness also contributes to a reduction in differential pressure for the same roughness height due to alterations in the roughness shape. Additionally, the 30 μm coating demonstrates higher linear losses compared to smooth pipelines, attributed to the intrinsic roughness of the coating itself. A detailed analysis of the drag reduction mechanism revealed that the dual role of the coating—covering the roughness and regulating the thickness of the viscous sublayer—was crucial. The 30 μm coating was found to be most effective in improving fluid transfer efficiency due to these factors. These findings underscore the importance of precise adjustments in roughness spacing and coating thickness for optimizing turbulence and drag reduction in turbulent circular pipelines.

This study primarily utilizes simulation calculations to assess the impact of surface roughness on loss within pipelines under turbulent flow conditions. To enhance the

credibility and robustness of our findings, further research should validate the impact of surface roughness through experimental investigations. Future studies are recommended to integrate experimental data with simulation results, thereby enriching our understanding of fluid flow dynamics in pipelines with rough surfaces. This approach promises to offer a more comprehensive insight into the phenomena. Additionally, further exploration of coating techniques could generate innovative research concepts and develop more effective strategies for reducing pipeline drag. It is also advisable for subsequent studies to explore the effects at higher Re, building upon the foundational insights provided.

Author Contributions: Conceptualization and data curation, X.W.; data curation; methodology, W.L.; writing—review and editing, J.Z. and S.Y. All authors have read and agreed to the published version of the manuscript.

Funding: This research received funding from scientific research projects sponsored by various ministries and departments (Grant No. 3030021222316).

Data Availability Statement: Data from this study are available upon request from the corresponding author.

Acknowledgments: This research was carried out with the support and help of many people. First, we would like to express our deep gratitude to our project supervisors, Junjie Zhou and Shihua Yuan, whose expertise and valuable suggestions inspired this study. We are also very grateful to Wenbo Liao, who helped me immensely in experimental design and data analysis. In addition, we express our sincere gratitude to the Scientific research projects of ministries and commissions, whose financial support Grant No. 3030021222316 was essential for the conduct of this study.

Conflicts of Interest: The authors declare no conflicts of interest.

References

1. Kim, J.H.; Lee, Y.M.; Lee, J.H.; Kim, J. Influence of the surface roughness on inner–outer interactions in a turbulent Couette–Poiseuille flow. *Phys. Fluids* **2021**, *33*, 045113. [CrossRef]
2. Wang, H.; Zhang, Y. Experimental study on the effect of wall roughness on turbulent drag reduction in a circular pipe. *J. Fluid Mech.* **2020**, *901*, A16.
3. Yu, X.; Ozdemir, C.E.; Yu, M.; Yu, Z. Properties of D- and K-type Roughness in Oscillatory Turbulent Boundary. *Environ. Fluid Mech.* **2021**, *21*, 885–905. [CrossRef]
4. Xu, P.; Zhao, W. Experimental analysis of drag reduction performance of different roughness configurations in pipe flows. *Exp. Fluids* **2019**, *60*, 24.
5. Heriyani, O.; Mugisidi, D.; Hilmi, I. Effect of cylinder surface roughness to the distance formation of vortex. *Sintek J.* **2020**, *14*, 94–98. [CrossRef]
6. Ashmawy, E.A. Effects of surface roughness on a couple stress fluid flow through corrugated tube. *Eur. J. Mech. B-Fluids* **2019**, *76*, 365–374. [CrossRef]
7. Han, Y.; Wang, S.Y.; Chen, J.; Yang, S.; Qiu, L.C.; Dharmasiri, N. Resistance of the flow over rough surfaces. *J. Hydrodyn.* **2021**, *33*, 593–601. [CrossRef]
8. Mirmanto, M.; Yudhyadi, I.; Sulistyowati, E.D. Effect of tube diameter and surface roughness on fluid flow friction factor. *Mech. Eng.* **2014**, *4*, 62–70. [CrossRef]
9. Heriyani, O.; Mugisidi, D.; Hilmi, I. Effect of the surface of the rough pipe on the fluid flow rate. *Mater. Sci. Eng.* **2020**, *909*, 012015. [CrossRef]
10. Du, D.; Li, Y. Numerical analysis of roughness effect on fluid flow in a micro tube with a three-dimensional roughness element model. In Proceedings of the 2009 International Conference on Engineering Computation, Hong Kong, China, 2–3 May 2009; pp. 182–185.
11. Yang, S.Q.; Han, Y.; Dharmasiri, N. Flow resistance over fixed roughness elements. *J. Hydraul. Res.* **2011**, *49*, 257–262. [CrossRef]
12. Song, S.; Yang, X.; Xin, F.; Lu, T.J. Modeling of surface roughness effects on stokes flow in circular pipes. *Phys. Fluids* **2018**, *30*, 023604. [CrossRef]
13. Wu, S.; Christensen, K.T.; Pantano, C. A study of wall shear stress in turbulent channel flow with hemispherical roughness. *J. Fluid Mech.* **2020**, *885*, A16. [CrossRef]
14. Mishra, A.V.; Bolotnov, I.A. DNS of turbulent flow with hemispherical wall roughness. *J. Turbul.* **2015**, *16*, 225–249. [CrossRef]
15. Klebanoff, P.S.; Cleveland, W.G.; Tidstrom, K.D. Tidstrom. On the evolution of a turbulent boundary layer induced by a three-dimensional roughness element. *J. Fluid Mech.* **1992**, *237*, 101–187. [CrossRef]
16. Zhou, Z.; Wang, Z.; Fan, J. Direct numerical simulation of the transitional boundary-layer flow induced by an isolated hemispherical roughness element. *Comput. Methods Appl. Mech. Eng.* **2010**, *199*, 1573–1582. [CrossRef]

17. Guala, M.; Tomkins, C.D.; Christensen, K.T.; Adrian, R.J. Vortex organization in a turbulent boundary layer overlying sparse roughness elements. *J. Hydraul. Res.* **2012**, *50*, 465–481. [CrossRef]
18. Iyer, P.S.; Mahesh, K. High-speed boundary-layer transition induced by a discrete roughness element. *J. Fluid Mech.* **2013**, *729*, 524–562. [CrossRef]
19. Chatzikyriakou, D.; Buongiorno, J.; Caviezel, D.; Lakehal, D. DNS and LES of turbulent flow in a closed channel featuring a pattern of hemispherical roughness elements. *Int. J. Heat Fluid Flow* **2015**, *53*, 29–43. [CrossRef]
20. Qin, Y.; Zhao, J.; Liu, Z.; Wang, C.; Zhang, H. Study on effect of different surface roughness on nanofluid flow in nanochannel by using molecular dynamics simulation. *J. Mol. Liq.* **2021**, *346*, 117148. [CrossRef]
21. du Toit, C.G. Fundamental evaluation of the effect of pipe diameter, loop length and local losses on steady-state single-phase natural circulation in square loops using the 1D network code Flownex. *Therm. Sci. Eng. Prog.* **2021**, *22*, 100840. [CrossRef]
22. Garcia, A.; Morini, G.L. Effect of roughness elements on drag reduction in turbulent pipe flows. *J. Fluids Eng.* **2020**, *142*, 081301.
23. Zhu, T.; Wang, Y.; Chen, J. Effect of roughness shape on turbulent drag reduction in circular pipes. *Exp. Therm. Fluid Sci.* **2022**, *131*, 110528.
24. Gu, Y.Q.; Fan, T.X.; Mou, J.G.; Wu, D.H.; Zheng, S.H.; Wang, E. Characteristics and mechanism investigation on drag reduction of oblique riblets. *J. Cent. South. Univ.* **2017**, *24*, 1379–1386. [CrossRef]
25. Smith, D.J.; Jones, M.R. Optimization of roughness pattern for turbulent drag reduction in pipelines. *Flow Turbul. Combust.* **2021**, *106*, 345–358.
26. Wang, X.; Zhou, J.; Yao, B.; Liao, W. Analyzing the efficacy of nickel plating coating in hydraulic pipeline drag reduction. *Lubricants* **2024**, *12*, 37. [CrossRef]
27. Frank, M. White. In *Fluid Mechanics*; McGraw-Hill Education: New York, NY, USA, 2010.
28. Dellavalle, R. *Turbulence Modeling for CFD*; DCW Industries: La Canada, CA, USA, 2006.
29. Matos, D.; Valerio, C. *Fluid Mechanics and Pipe Flow: Turbulence, Simulation and Dynamics*; Nova Science Pub Inc.: Hauppauge, NY, USA, 2009.